Proceeding Paper

The Use of Ultra-High Resolution UAV Lidar Infrared Intensity for Enhancing Coastal Cover Classification †

Antoine Collin [1,*] , Dorothée James [1] , Régis Gallon [2,3] , Emmanuel Poizot [2,3] and Eric Feunteun [1,4]

1 Coastal GeoEcological Lab, Ecole Pratique des Hautes Etudes, PSL University, 35800 Dinard, France; dorothee.james@ephe.psl.eu (D.J.); eric.feunteun@ephe.psl.eu (E.F.)

2 Conservatoire National des Arts et Métiers, INTECHMER, 50100 Cherbourg-en-Cotentin, France; regis.gallon@lecnam.net (R.G.); emmanuel.poizot@lecnam.net (E.P.)

3 UNICAEN, Laboratoire des Sciences Appliquées de Cherbourg, Normandie University, EA 4253, 50100 Cherbourg-en-Cotentin, France

4 UMR BOREA (MNHN, CNRS, SU, IRD, UCN, UA), 35800 Dinard, France

* Correspondence: antoine.collin@ephe.psl.eu

† Presented at the 5th International Electronic Conference on Remote Sensing, 7–21 November 2023; Available online: https://ecrs2023.sciforum.net/.

Abstract: Coastal areas gather increasing hazards, exposures, and vulnerabilities in the context of anthropogenic changes. Understanding their spatial responses to acute and chronic drivers requires ultra-high spatial resolution that can only be achieved by UAV-based sensors. UAV lasergrammetry constitutes, to date, the best observation of the xyz variables in terms of resolution, precision, and accuracy, allowing coastal areas to be reliably mapped. However, the use of lidar reflectivity (or intensity) remains poorly examined for mapping purposes. The added value of the lidar-derived near-infrared (NIR) was estimated by comparing the classification results of nine coastal habitats based on the blue–green–red (BGR) passive and BGR-NIR passive–active datasets. A gain of 4.14% was found at the landscape level, while habitat-scaled improvements were highlighted for the "salt marsh" and "soil" habitats (4 and 4.56% for producer's accuracy, PA, and user's accuracy, UA; and 8.95 and 9.48% for PA and UA, respectively).

Keywords: salt marsh; lidar near-infrared intensity; DJI L1

1. Introduction

Coastal areas play a key role in the adaptation of ocean-climate change due to their land–sea interface [1]. The mapping and monitoring of their use and cover are crucial to understanding where the most exposed and vulnerable zones are located and how to manage them in a sustainable way [2]. The finest spatial resolution possible is required to empower the diagnosis and prognosis of coastal objects subject to current and future erosion and/or submersion risks. To date, unmanned aerial vehicles (UAVs) consist of the best platforms to bear sensors capable of providing centimeter-scale 2D and 3D coastal information [3]. The active lidar instrument scans coastal landscapes at a rate of hundreds of thousands of points per second, propagating at the speed of light [4]. UAV-based lidar products enable the best accuracy and precision in xyz data among the airborne/spaceborne tools. However, lidar intensity remains poorly harnessed in Earth observation from satellite to drone, despite its obvious added value in terms of spectral information [5].

This study aims to assess the contribution of the UAV-based lidar-derived near-infrared (NIR) intensity to the overall accuracy (OA) and kappa coefficient (κ) of the classification of a coastal landscape, provided with nine representative natural, semi-natural, and anthropogenic habitats. The lidar NIR contribution is quantified in the light of blue–green–red (BGR) passive imagery, whose camera is co-located with the lidar sensor.

2. Methodology

2.1. Study Site

The study site is located along the bay of Mont Saint-Michel, midway between the most extended salt marshes in northern France and rural polders (Figure 1).

Figure 1. Blue–green–red composite imagery of the study site and its global location (11,385 × 5538 pixels; 0.01 m pixel size; 23,626,927 points).

This site was selected based on the diversity of the habitats, namely salt marsh, grass, dry grass, shrub, tree, soil, sediment, road, and car (Table 1). Every class was represented by 4600 pixels, which were split into 2300 calibration and 2300 validation pixels. Both sub-datasets were spatially disjointed to avoid spatial autocorrelation. A total of 41,400 pixels were therefore used for, first, training the probabilistic maximum likelihood learner, then for testing its predictability.

Table 1. Habitat name, description, and blue–green–red derived thumbnails.

Habitat Name	Habitat Description	Habitat Thumbnail
Salt marsh	High-salt marsh herbaceous stratum	
Grass	Terrestrial herbaceous stratum	
Dry grass	Dried terrestrial herbaceous stratum	
Shrub	Terrestrial arbustive stratum	
Tree	Terrestrial arborescent stratum	
Soil	Mixed organic/mineral bare ground	

Table 1. *Cont.*

Habitat Name	Habitat Description	Habitat Thumbnail
Sediment	Mineral-bare ground	
Road	Tar anthropogenic infrastructure	
Car	Anthropogenic vehicle	

2.2. Drone Lidar Flight

The lidar drone mission was realized on 5 June 2023 using a Zenmuse L1 sensor (DJI, Shenzhen, China) mounted on a DJI Matrice 300 RTK quadcopter (DJI, Shenzhen, China) linked with a DJI D-RTK2 high precision Global Navigation Satellite System (GNSS) station base. The flight mission followed these navigational parameters: 50 m height, 4 m/s speed, 12 min time, 2.04 km path length, 0.30 km^2, 233 BGR pictures, and 0.013 m ground sample distance.

The Zenmuse L1 sensor is designed to have a 905 nm Livox Avia laser, a 200 Hz inertial measurement unit, and a 1-inch RGB camera (20 Mp), all mounted on a 3-axis gimbal provided with a DJI Skyport (DJI, Shenzhen, China), enabling the synchronization of the lidar RTK positioning with the Matrice 300 RTK system. The point sampling rate was fixed at 240 kHz in the dual return mode, and the line scanning pattern was selected (repetitive field-of-view: 70.4° horizontal × 4.5° vertical). The lidar mission followed these specific parameters: 80% front overlapping, 70% side overlapping, and an average density point of 2 477 points/m^2. The DJI native (but proprietary) lidar format was implemented into DJI Terra (DJI, Shenzhen, China) to obtain the las format in the local datum RGF93, projected in Lambert 93, along the IGN69 altimetry. The mean NIR intensity was rasterized at 0.01 m from the resulting point cloud (Figure 2).
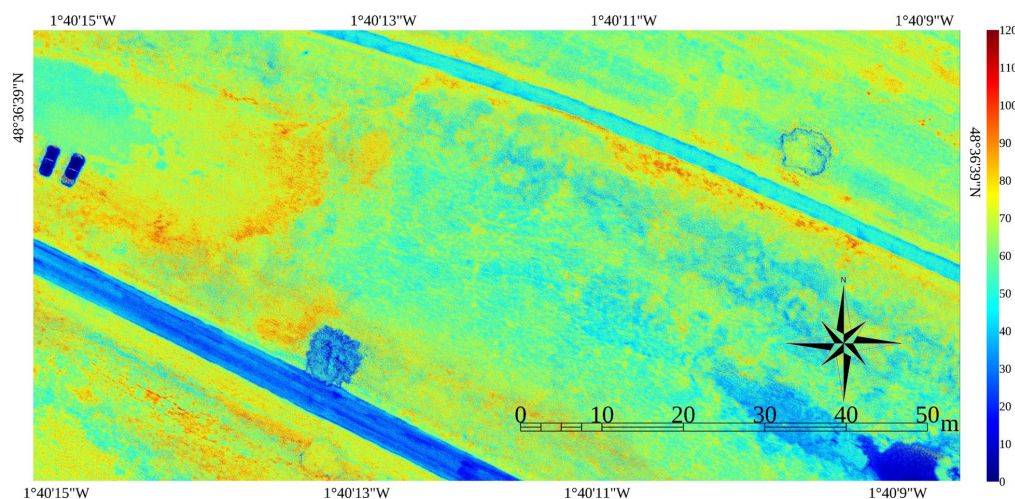
Figure 2. Infrared lidar-derived near-infrared imagery of the study site (11,385 × 5538 pixels; 0.01 m pixel size; 23,626,927 points).

3. Results and Discussion

3.1. Landscape Scale

The OA and κ were derived from the confusion matrices established from the validation datasets of the BGR (Table 2) and BGR-NIR (Table 3) classifications. OA and κ

reached 84.57% and 0.8264 for the BGR and 88.71% and 0.8730 for the BGR-NIR datasets, respectively (Figure 3).

Table 2. Confusion matrix derived from the blue–green–red classification.

	Salt Marsh	Grass	Dry Grass	Shrub	Tree	Soil	Sediment	Road	Car
Salt marsh	1955	0	0	0	0	0	0	0	0
Grass	0	2298	0	0	0	0	0	0	0
Dry grass	334	2	1966	157	368	0	42	0	0
Shrub	0	0	240	2143	0	0	0	0	793
Tree	0	0	88	0	1932	0	0	0	0
Soil	0	0	0	0	0	2176	2	133	0
Sediment	0	0	3	0	0	78	2138	776	0
Road	0	0	3	0	0	46	118	1391	0
Car	11	0	0	0	0	0	0	0	1507

Table 3. Confusion matrix derived from the blue–green–red + lidar-derived near-infrared classification.

	Salt Marsh	Grass	Dry Grass	Shrub	Tree	Soil	Sediment	Road	Car
Salt marsh	2250	0	0	0	0	0	0	0	14
Grass	0	2298	0	0	0	0	0	0	0
Dry grass	39	2	1920	145	108	2	54		779
Shrub	0	0	236	2155	0	0	0	0	0
Tree	0	0	141	0	2192	0	0	0	0
Soil	0	0	0	0	0	2214	2	78	0
Sediment	0	0	3	0	0	78	2230	625	0
Road	0	0	0	0	0	6	14	1597	0
Car	11	0	0	0	0	0	0	0	1507
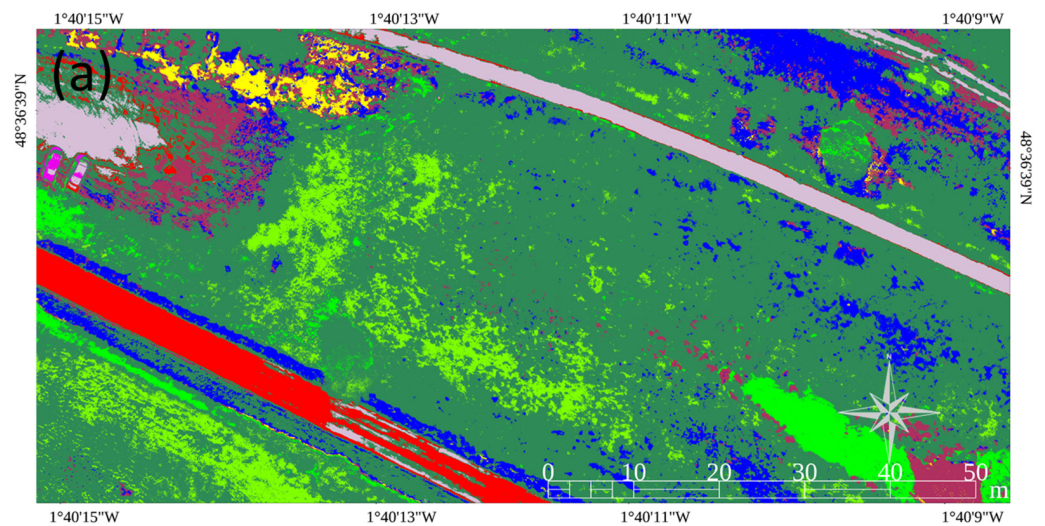
Figure 3. *Cont.*
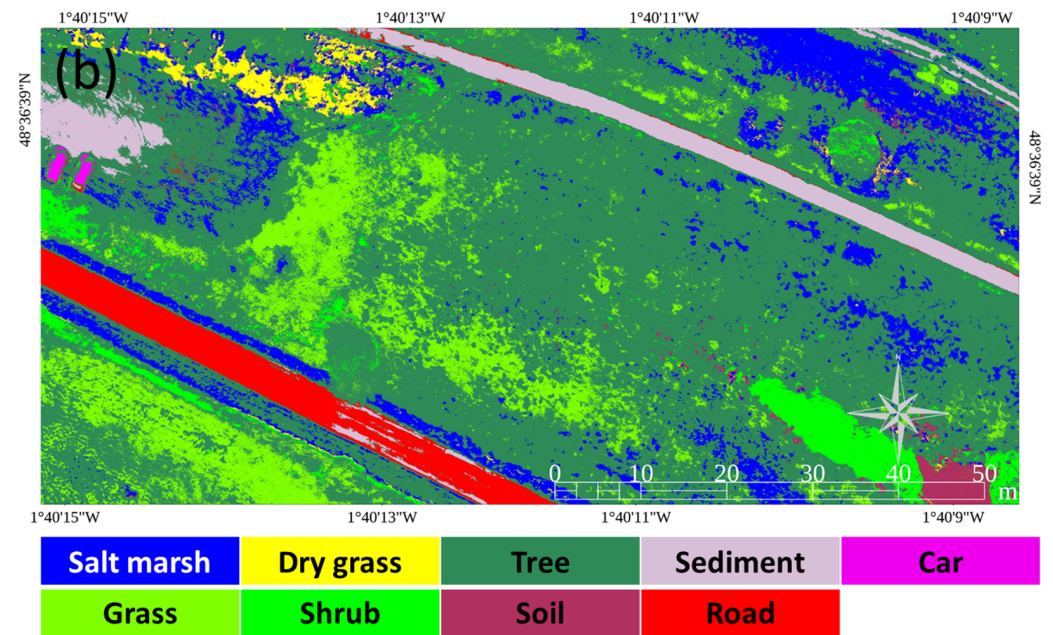
Figure 3. Classification of the nine classes in the coastal landscape based on (**a**) blue–green–red imagery and (**b**) lidar-derived near-infrared + blue–green–red imageries (11,385 × 5538 pixels, 0.01 m pixel size).

3.2. Habitat Scale

Regarding the producer's accuracy (PA), the habitats that most benefited from the NIR addition were "road", "grass", and "soil", whereas "tree" lost a little detection.

About the user's accuracy (UA), "soil", "tree", and "salt marsh" gained in discrimination, whereas "road" and "grass" were less classified (Table 4).

Table 4. Results of the producer's accuracy and user's accuracy differences between BGR and BGR-NIR classifications.

Habitat Name	Producer's Accuracy	User's Accuracy
Salt marsh	4	4.56
Grass	11.3	−1.68
Dry grass	1.65	2.35
Shrub	0.53	0.2
Tree	−2	9.28
Soil	8.95	9.48
Sediment	0	0
Road	12.83	−0.62
Car	0	0

The consistent augmentation for "salt marsh" and "soil" might be explained by the higher and lower reflectance in the NIR spectrum, respectively. High salt marsh vegetation, such as *Puccinellia*, *Festuca*, *Aster*, *Limione*, or *Elymus* genera, displays a tangible higher NIR reflectance in the summer season [6], while the "soil" investigated here corresponded to the transitional wet-to-dry area just above a pond, thus the lower NIR reflectance due to the moisture.

4. Conclusions

The contribution of the UAV-borne lidar-derived NIR intensity to the classification of a coastal landscape (provided with nine representative habitats) was evaluated by comparing OA, PA, and UA results associated with a passive BGR dataset and a combination of a passive–active BGR-NIR dataset using a probabilistic maximum likelihood classifier. At

the landscape level, the addition of the lidar NIR intensity to the BGR reference increased OA by 4.14%. At the habitat level, "salt marsh" and "soil" gained 4 and 8.95% in PA, respectively, and 4.56 and 9.48% in UA, respectively. It is therefore recommended to add the lidar-derived intensity into classification when front and side overlaps at least reach 80 and 70%, respectively.

Author Contributions: Conceptualization, A.C., D.J., R.G., E.P. and E.F.; methodology, A.C., D.J., R.G., E.P. and E.F.; software, A.C., D.J., R.G., E.P. and E.F.; validation, A.C., D.J., R.G., E.P. and E.F.; formal analysis, A.C., D.J., R.G., E.P. and E.F.; investigation, A.C., D.J., R.G., E.P. and E.F.; resources, A.C., D.J., R.G., E.P. and E.F.; data curation, A.C., D.J., R.G., E.P. and E.F.; writing—original draft preparation, A.C., D.J., R.G., E.P. and E.F.; writing—review and editing, A.C., D.J., R.G., E.P. and E.F.; visualization, A.C., D.J., R.G., E.P. and E.F.; supervision, A.C., D.J., R.G., E.P. and E.F.; project administration, A.C., D.J., R.G., E.P. and E.F.; funding acquisition, A.C., D.J., R.G., E.P. and E.F. All authors have read and agreed to the published version of the manuscript.

Funding: This research received no external funding.

Institutional Review Board Statement: Not applicable.

Informed Consent Statement: Not applicable.

Data Availability Statement: The datasets presented in this article are not readily available because the data are part of an ongoing study. Requests to access the datasets should be directed to DJ.

Acknowledgments: The authors are grateful to the French Office for Biodiversity for authorizing the UAV flights over natural and semi-natural habitats.

Conflicts of Interest: The authors declare no conflict of interest. The funders had no role in the design of the study, in the collection, analysis, or interpretation of data, in the writing of the manuscript, or in the decision to publish the results.

References

1. Toimil, A.; Losada, I.J.; Nicholls, R.J.; Dalrymple, R.A.; Stive, M.J. Addressing the challenges of climate change risks and adaptation in coastal areas: A review. *Coast. Eng.* **2020**, *156*, 103611. [CrossRef]
2. Bukvic, A.; Rohat, G.; Apotsos, A.; de Sherbinin, A. A systematic review of coastal vulnerability mapping. *Sustainability* **2020**, *12*, 2822. [CrossRef]
3. Collin, A.; James, D.; Mury, A.; Letard, M.; Houet, T.; Gloria, H.; Feunteun, E. Multiscale Spatiotemporal NDVI Mapping of Salt Marshes Using Sentinel-2, Dove, and UAV Imagery in the Bay of Mont-Saint-Michel, France. In *European Spatial Data for Coastal and Marine Remote Sensing*; Springer International Publishing: Cham, Switzerland; New York, NY, USA, 2022; pp. 17–38.
4. Collin, A.; Pastol, Y.; Letard, M.; Le Goff, L.; Guillaudeau, J.; James, D.; Feunteun, E. Increasing the Nature-Based Coastal Protection Using Bathymetric Lidar, Terrain Classification, Network Modelling: Reefs of Saint-Malo's Lagoon? In *European Spatial Data for Coastal and Marine Remote Sensing*; Springer International Publishing: Cham, Switzerland; New York, NY, USA, 2022; pp. 235–241.
5. Collin, A.; Ramambason, C.; Pastol, Y.; Casella, E.; Rovere, A.; Thiault, L.; Davies, N. Very high resolution mapping of coral reef state using airborne bathymetric LiDAR surface-intensity and drone imagery. *Int. J. Remote Sens.* **2018**, *39*, 5676–5688. [CrossRef]
6. Mury, A.; Collin, A.; Etienne, S.; Jeanson, M. Wave attenuation service by intertidal coastal ecogeosystems in the Bay of Mont-Saint-Michel, France: Review and meta-analysis. In *Estuaries and Coastal Zones in Times of Global Change*; Springer Water, Springer: Singapore, 2020; pp. 555–572.